

Interfacial slip in sheared polymer blends

Tak Shing Lo,¹ Maja Mihajlovic,² Yitzhak Shnidman,^{3,5,*} Wentao Li,⁴ and Dilip Gersappe^{4,5}

¹The Levich Institute, City College of CUNY, New York, New York 10031, USA

²Department of Chemistry, City College of CUNY, New York, New York 10031, USA

³Department of Engineering Science and Physics, College of Staten Island of CUNY, Staten Island, New York 10314, USA

⁴Department of Materials Science and Engineering, Stony Brook University, Stony Brook, New York 11794, USA

⁵The NSF MRSEC on Polymers at Engineered Interfaces, Stony Brook University, Stony Brook, New York 11794, USA

(Received 4 May 2005; published 3 October 2005; publisher error corrected 6 October 2005)

We have developed a dynamic self-consistent field theory, without any adjustable parameters, for unentangled polymer blends under shear. Our model accounts for the interaction between polymers, and enables one to compute the evolution of the local rheology, microstructure, and the conformations of the polymer chains under shear self-consistently. We use this model to study the interfacial dynamics in sheared polymer blends and make a quantitative comparison between this model and molecular dynamics simulations. We find good agreement between the two methods.

DOI: [10.1103/PhysRevE.72.040801](https://doi.org/10.1103/PhysRevE.72.040801)

PACS number(s): 83.80.Tc, 83.10.Rs, 83.50.Lh

Understanding and modeling the interplay between interfacial properties and chain conformations at polymer fluid interfaces is of great fundamental and practical importance. Self-consistent field (SCF) theory has been very useful for modeling equilibrium properties of such interfaces [1]. In contrast, interfacial dynamics and rheology in polymer fluids driven out of equilibrium by applied stresses are still not well understood.

We have recently developed a dynamic self-consistent field (DSCF) theory [2] by combining the lattice random-walk formalism of Scheutjens and Fler's static SCF model [1] and a convective-diffusive lattice gas model for simple compressible fluids [3]. As in static SCF theory, the distribution of free segments interacting with a self-consistent field representing adjacent connected segments and walls is approximated by a product of free segment (one-body) probabilities. The effect of flow on ideal chain conformations is modeled with elastic dumbbells, and related to stepping probabilities in a random walk. Free segment and stepping probabilities generate statistical weights for chain conformations in a self-consistent field, and determine local volume fractions of connected segments. Flux balance across a unit lattice cell yields mean-field transport equations for free segment probabilities and momentum densities. Diffusive and viscous contributions to the fluxes arise from segmental hops that are modeled as a Markov process. Hopping transition rates depend on the changes in the free energy, reflecting segmental interactions, kinetic energy, and entropic contributions accounting for chain deformation under flow. This dynamic mean-field theory for inhomogeneous polymer fluids couples self-consistently the effects of flow, segmental and wall interactions, and compressibility on chain conformations, composition, transport, and rheology in interfacial regions at the Kuhn length scale, which is necessary to resolve interfacial properties of typical polymer interfaces. This makes it different from other recently proposed approaches

[4]. In this paper, we focus on the interfacial dynamics of a symmetric polymer blend in the unentangled regime. We use the DSCF model to predict the velocity slip, chain conformations, and the reduction of shear viscosity across the interface between the coexisting polymer phases, and compare our results with molecular dynamics (MD) simulations.

We consider a blend of two immiscible homopolymer species A and B consisting of linear chains of N^A and N^B segments, respectively. The fluid is confined between two parallel walls normal to the z axis in a Cartesian coordinate system at temperature T . The interface between the two polymers is parallel to, and is centered midway between, the two walls. The walls move at equal and opposite velocities along the x axis. We discretize the space between the two walls into triangular lattice layers parallel to the walls, stacked in a fcc lattice arrangement. The fluid system considered here is invariant under lattice translations in the xy plane, and we simplify the DSCF equations utilizing this symmetry (see [2] for details).

Let P_i^α , ϕ_i^α , and \mathbf{g}_i^α be the free segment probability, segmental volume fraction, and segmental momentum density of species α ($\alpha=A$ or B) in each layer i ($i=1,2,\dots,L$), respectively. The free segment probabilities and the segmental momentum densities \mathbf{g}_i^α evolve according to

$$dP_i^\alpha/dt = -\nabla \cdot (P_i^\alpha \mathbf{u}_i) - [(\mathbf{j}_i^\alpha - \mathbf{j}_{i-1}^\alpha)/\sqrt{2/3}a] \cdot \hat{\mathbf{z}}, \quad (1)$$

and

$$\begin{aligned} \frac{d\mathbf{g}_i^\alpha}{dt} = & -\nabla \cdot (\mathbf{g}_i^\alpha \mathbf{u}_i + \boldsymbol{\varepsilon}_i^\alpha) - \left(\frac{\boldsymbol{\pi}_i^\alpha - \boldsymbol{\pi}_{i-1}^\alpha}{\sqrt{2/3}a} \right) \cdot \hat{\mathbf{z}} \\ & - \frac{\phi_i^\alpha}{wP_i^\alpha} (\zeta_{i,i+1}^\alpha \mathbf{j}_i^\alpha + \zeta_{i,i-1}^\alpha \mathbf{j}_{i-1}^\alpha), \end{aligned} \quad (2)$$

which are obtained by applying mass and momentum conservation laws to a rectangular control volume of $w=a^3/\sqrt{2}$ centered at a site in layer i . Here $\zeta_{i,i\pm 1}^\alpha$ is the locally averaged segmental friction coefficient of species α (see [2] for details) and $\mathbf{u}_i = (\mathbf{g}_i^A + \mathbf{g}_i^B)w/(m^A \phi_i^A + m^B \phi_i^B)$ is the mass averaged velocity at a site in layer i , where m^α is the segmental mass of species α . The tensor $-\boldsymbol{\varepsilon}_i^\alpha$ in Eq. (2) represents the

*Corresponding author. Electronic address: shnidman@mail.csi.cuny.edu

elastic contribution to the stress and is defined in [2]. Let $D_{i,i+1}^\alpha = k_B T / N^\alpha \zeta_{i,i+1}^\alpha$ and $\nu_{i,i+1}^\alpha = \zeta_{i,i+1}^\alpha a^2 / 24m^\alpha$ be the locally averaged self-diffusion coefficient and kinematic viscosity of species α , $\phi_i = \phi_i^A + \phi_i^B$ be the total polymer volume fraction at a site in layer i , and $\bar{\phi} = L^{-1} \sum_{i=1}^L \phi_i$. The diffusive free segment probability current and the viscous stress tensor at the midplane between layers i and $i+1$ in Eqs. (1) and (2) are given by

$$\mathbf{j}_i^\alpha = 3 \sqrt{\frac{2}{3}} \frac{(1 - \delta_{i+1,L})(1 - \delta_{i,L})}{(1 - \bar{\phi})} \frac{D_{i,i+1}^\alpha}{a} [P_i^\alpha (1 - \phi_{i+1}) \times \varphi(\Delta(H_i^\alpha)/k_B T) - P_{i+1}^\alpha (1 - \phi_i) \varphi(-\Delta(H_i^\alpha)/k_B T)] \hat{\mathbf{z}}, \quad (3)$$

and

$$\boldsymbol{\pi}_i^\alpha = 3 \sqrt{\frac{2}{3}} \frac{(1 - \delta_{i+1,L})(1 - \delta_{i,L})}{(1 - \bar{\phi})} \frac{m^\alpha \nu_{i,i+1}^\alpha}{w a} \left[\phi_i^\alpha \mathbf{u}_i (1 - \phi_{i+1}) \times \varphi\left(\frac{\Delta(H_i^\alpha)}{k_B T}\right) - \phi_{i+1}^\alpha \mathbf{u}_{i+1} (1 - \phi_i) \varphi\left(\frac{-\Delta(H_i^\alpha)}{k_B T}\right) \right] \hat{\mathbf{z}}. \quad (4)$$

In Eqs. (3) and (4), φ is the Kawasaki transition rate function $\varphi(h) = 2/(1 + e^h)$ [5] that satisfies the local detailed balance, and $\Delta(H_i^\alpha) = \langle H_{i+1}^\alpha \rangle - \langle H_i^\alpha \rangle$ is the free energy change due to a hop of a segment of species α from layer i to $i+1$. A segment of species α in layer i is subject to the self-consistent potential

$$\langle H_i^\alpha \rangle = \sum_{\beta=A,B} \frac{(1 - \delta_{\alpha\beta})}{2} \chi_{AB} \langle \phi_i^\beta \rangle + \chi_s^\alpha (\delta_{i1} + \delta_{iL}) + \frac{m^\alpha}{2} \phi_i^\alpha \mathbf{u}_i^2 - (\phi_i^\alpha k_B T / 2N^\alpha) (\text{Tr} \{ \boldsymbol{\delta} - [3/(N^\alpha - 1)a^2] \mathbf{S}_i^\alpha \}) + \ln \det \{ [3/(N^\alpha - 1)a^2] \mathbf{S}_i^\alpha \}, \quad (5)$$

where χ_{AB} is the segment-segment interaction parameter for species A and B , and χ_s^α is the segment-wall interaction parameter of a segment of species α . In Eq. (5), the double angular brackets represent the summation over all nearest neighbors of a site in layer i , and \mathbf{S}_i^α is the second moment of the end-to-end vector of an ideal (noninteracting) α -type chain under flow, with its center of mass being in the i th layer. The last two terms in Eq. (5) are contributions from the kinetic energy and the free energy change due to the stretching of the chains.

The conformations of interacting polymer chains are generated by lattice random walks in the self-consistent field of Eq. (5). According to [1], the segmental volume fraction is obtained from the free segment probability by

$$\phi_i^\alpha = \frac{\bar{\phi}^\alpha L}{N^\alpha \sum_{j=1}^{N^\alpha} P_j^\alpha(N^\alpha)} \sum_{s=1}^{N^\alpha} \frac{P_i^\alpha(s) P_i^\alpha(N^\alpha - s + 1)}{P_i^\alpha / (1 - P_i^A - P_i^B)}, \quad (6)$$

where

$$P_i^\alpha(s) = P_i^\alpha [\lambda_{+,i-1}^\alpha P_{i-1}^\alpha(s-1) + \lambda_{0,i}^\alpha P_i^\alpha(s-1) + \lambda_{-,i+1}^\alpha P_{i+1}^\alpha(s-1)] / (1 - P_i^A - P_i^B) \quad (7)$$

for $s=2, 3, \dots, N^\alpha$ and $P_i^\alpha(1) = P_i^\alpha / (1 - P_i^A - P_i^B)$. In Eq. (6),

$\bar{\phi}^\alpha$ is the average volume fraction of species α in the system and in Eq. (7), $\lambda_{\pm,i}^\alpha$ is the stepping probability of an α -type segment in an ideal chain from layer i to layer $i \pm 1$, whereas $\lambda_{0,i}^\alpha$ is the stepping probability from a site in layer i to a nearest neighbor in the same layer. In contrast to the static SCF theory, these probabilities are now time dependent and anisotropic, and are related to the components of \mathbf{S}_i^α through the random-walk picture (see [2]).

Finally, \mathbf{S}_i^α evolves according to

$$\frac{D\mathbf{S}_i^\alpha}{Dt} - (\nabla \mathbf{u}_i)^T \cdot \mathbf{S}_i^\alpha - \mathbf{S}_i^\alpha \cdot (\nabla \mathbf{u}_i) = - \frac{1}{\tau_{db,i}^\alpha} \left\{ \frac{\mathbf{S}_i^\alpha}{1 - \text{Tr} \mathbf{S}_i^\alpha / [N^\alpha(N^\alpha - 1)a^2]} - \frac{N^\alpha a^2}{3} \boldsymbol{\delta} \right\}, \quad (8)$$

which is the constitutive equation of a finitely extensible, nonlinear elastic dumbbell, using the self-averaging Peterlin approximation (the FENE-P model) [6,7], but with the value of the spring constant chosen in such a way that \mathbf{S}_i^α reverts to the Hookean dumbbell value in equilibrium. In Eq. (8), $\tau_{db,i}^\alpha = (N^\alpha a)^2 \zeta_i^\alpha / 24k_B T$ is the local dumbbell relaxation time where ζ_i^α is the local segmental friction coefficient of species α , which is related to the one in the bulk through the Doolittle's law [8] (see [2] for details).

In the actual computation, all spatial derivatives are approximated by using finite difference formulas. Under suitable boundary conditions, Eqs. (1), (2), and (8) form a closed system of ordinary differential equations, which is solved numerically.

Henceforth we focus on symmetric blends, i.e., $N^A = N^B = N$, $m^A = m^B = m$. The two polymers A and B have the same density and segmental friction coefficient. We also set $\chi_s^A = \chi_s^B = 0$. We shall compare the numerical solutions of the DSCF equations with molecular dynamics (MD) simulations of a similar system. The details of the model and the method of the MD simulation that we used can be found in [9]. In MD, the characteristic energy (ϵ), time (τ), and length (σ), and the segmental mass (m) are related by $\tau = \sigma \sqrt{m/\epsilon}$. As in [9], we set the temperature in our MD simulations by $\epsilon = k_B T / 1.1$.

In order to compare our model to MD simulations, we have to establish the relationships between the model parameters in the DSCF theory and those in MD. The Kuhn length in the MD simulations is estimated to be $a \approx 1.3\sigma$ [9], hence, one Kuhn segment is equivalent to 1.3 beads in MD. The interaction parameter χ_{AB} is obtained by fitting the equilibrium density profiles calculated from DSCF theory to the ones obtained from MD. After accounting for capillary wave broadening of the intrinsic profiles in MD simulations [10], this gives $12\chi_{AB}/k_B T \approx 1.1$. The segmental friction coefficient in the bulk is obtained by comparing the self-diffusion constants calculated from MD to the one in our model. The segmental mass in our model is identical to the one used in MD. All the other DSCF parameters can be expressed as combinations of the bulk segmental friction coefficient, the Kuhn length a , and χ_{AB} . In the simulations, we set $\bar{\phi}^A = \bar{\phi}^B$ and the overall polymer volume fraction averaged over the simulation box to $\bar{\phi} = \bar{\phi}^A + \bar{\phi}^B = 0.85$. This average volume

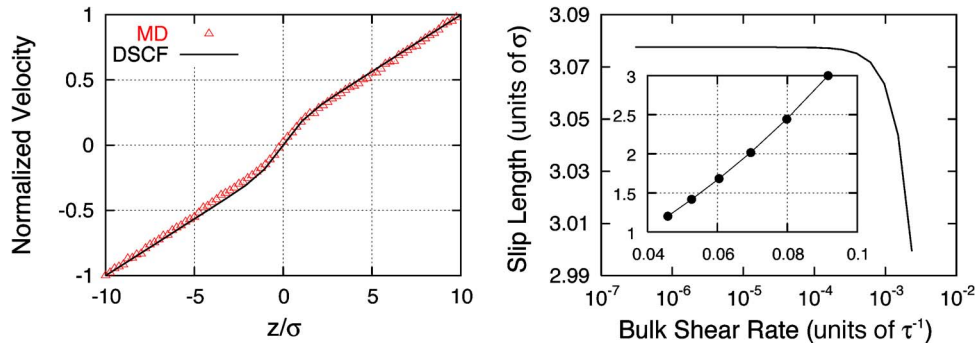


FIG. 1. (Color online) Left: Steady-state shear velocity profile for $N=12$ obtained from DSCF at bulk shear rate $2.36 \times 10^{-3} \tau^{-1}$ and MD at bulk shear rate $4.04 \times 10^{-3} \tau^{-1}$. The velocity is normalized by the velocity at $z=10\sigma$. Right: Variation of the slip length with the shear rate and with χ_{AB} for $N=12$ obtained from DSCF. The inset shows the slip length in σ versus $\chi_{AB}/k_B T$ at the nominal shear rate $2.75 \times 10^{-3} \tau^{-1}$.

fraction is used both in the DSCF model and MD simulations.

As the first test of the DSCF model, we calculated the steady-state velocity profiles and the local viscosities between the walls under shear for different chain lengths, and compared them with the MD results. The steady state is obtained by integrating the DSCF equations of motion in time under a constant rate for shearing the two walls (nominal shear rate), starting from equilibrium.

The shear velocity profile (defined as the local mass-averaged velocity) across the polymer-polymer interface in the middle of the channel from our model for $N=12$ is shown in the left panel of Fig. 1. The result from MD simulations using chains of 16 beads is also shown. Note that a kink representing a velocity slip at the interface is observed in both the DSCF and MD results. This interfacial slip phenomenon was first predicted using a scaling argument [11]. Subsequently, it was modeled with an approximate constitutive equation for incompressible polymer blends [12], and confirmed both by MD simulations [13] and experimental studies [14]. In this paper, the shear rates at which the DSCF results are obtained are lower than those in MD. This is because the current DSCF model fails at higher shear rates (though it covers most experimentally accessible shear rates), but MD simulations at lower shear rates are not computationally feasible. However, such a comparison is meaningful because these shear rates are still well into the Newtonian regime where shear thinning is negligible both in the bulk and at the interface [15].

To quantify the interfacial slip, we calculated the slip

length, which is defined as twice the magnitude of the x intercept of the straight line obtained from a linear fit to the linear part of the steady-state velocity profile. The results are shown in the right panel of Fig. 1. Our model shows a slight decrease in the slip length as the shear rate increases. We verified this result by performing MD simulations of the same system at two different bulk shear rates: one at $4.04 \times 10^{-3} \tau^{-1}$ and the other one at $8.27 \times 10^{-3} \tau^{-1}$. The slip lengths were found to be 1.95σ and 1.22σ , respectively. The trend is the same as the one predicted by the DSCF model. We also calculated the slip length as a function of χ_{AB} at a fixed nominal shear rate, and the result is shown in the inset of the same figure. It shows that the slip length increases as the strength of the segment-segment interaction increases. A similar qualitative trend was also observed by using MD in earlier studies [13].

We also calculated the second moment (S_{int}) of the end-to-end vector of the interacting polymer chains (not to be confused with the second moment of the end-to-end vector of the ideal chains) at steady state by performing a Monte Carlo simulation of lattice random walks in a self-consistent field representing conformations of interacting chains under shear. The transition rates used in the Monte Carlo simulation were constructed using the stepping and free segment probabilities from the DSCF theory. DSCF results for S_{int} of single chains are averaged with respect to the number density of chains of both species that are centered at each layer, and compared with similarly averaged MD results in Fig. 2. In the bulk, we have good agreement between the two simulations. The slight difference can be accounted for by the dif-

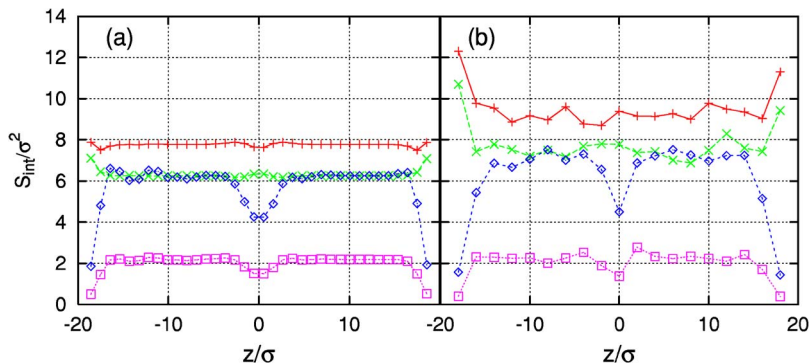


FIG. 2. (Color online) Second moment of the end-to-end distance for $N=12$ obtained from (a) DSCF at the bulk shear rate $2.36 \times 10^{-3} \tau^{-1}$, and (b) MD at bulk shear rate $4.04 \times 10^{-3} \tau^{-1}$. (+: S_{xx} , \times : S_{yy} , \diamond : S_{zz} , \square : S_{xz} .)

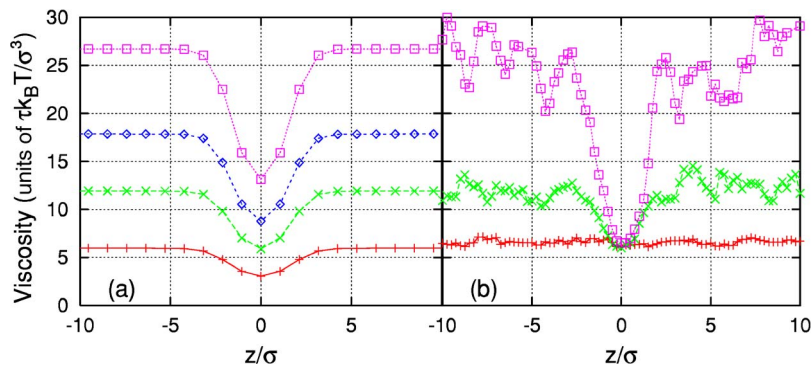


FIG. 3. (Color online) Steady-state shear viscosity profiles across the polymer-polymer interface for different chain lengths obtained from (a) DSCF at the nominal shear rate $6.24 \times 10^{-4} \tau^{-1}$, and (b) MD at various nominal shear rates. (+: $N=6$, \times : $N=12$, \diamond : $N=18$, \square : $N=24$.)

ference in the shear rates. In the interfacial region, our model predicts the same trend as in MD. Similar results were also obtained in [15] using MD.

When traversing a planar interface normal to the z axis, the variation of the self-consistent potential field H_r^α across the interface is dominated by unfavorable interactions between the two species, and thus closely resembles that of ϕ_r^β , giving rise to forces $\mathbf{F}_r^\alpha = -\nabla H_r^\alpha$. The evolution equation for $\mathbf{S}_{\text{int}}^\alpha$ of a Hookean dumbbell in an incompressible flow at a constant shear rate $\dot{\gamma}$, with external forces \mathbf{F}_1^α and \mathbf{F}_2^α exerted on the two beads separated by an end-to-end vector \mathbf{Q}_r^α , can be obtained by adding the term $(1/\xi_r^\alpha) \langle (\mathbf{F}_2^\alpha - \mathbf{F}_1^\alpha) \mathbf{Q}_r^\alpha + \mathbf{Q}_r^\alpha (\mathbf{F}_2^\alpha - \mathbf{F}_1^\alpha) \rangle$ to the right-hand side of the Hookean version of Eq. (8) (see p. 63 of [6]), where ξ_r^α is the chain friction coefficient. Using $\mathbf{F}_2^\alpha - \mathbf{F}_1^\alpha \approx \nabla \mathbf{F}_r^\alpha \cdot \mathbf{Q}_r^\alpha = -\nabla \nabla H_r^\alpha \cdot \mathbf{Q}_r^\alpha$, the only non-vanishing component of $\nabla \nabla H_r^\alpha$ is $\partial_z^2 H_r^\alpha \equiv -(\xi_r^\alpha / \tau_{db}) \Delta_r^\alpha$. The steady-state solution of this simplified model is $S_{yy}^\alpha = (N^\alpha - 1)a^2/3$, $S_{zz}^\alpha = S_{yy}^\alpha / (1 + 2\Delta_r^\alpha)$, $S_{xz}^\alpha = \dot{\gamma} \tau_{db} S_{zz}^\alpha / (1 + \Delta_r^\alpha)$, $S_{xx}^\alpha = S_{yy}^\alpha + 2\dot{\gamma} \tau_{db} S_{xz}^\alpha$ and $S_{xy}^\alpha = S_{yz}^\alpha = 0$. It indicates that steady shear leads to $S_{xz}^\alpha \neq 0$ and $S_{xx}^\alpha > S_{yy}^\alpha$ in the bulk regions, but the interfacial variations in S_{xx}^α , S_{zz}^α and S_{xz}^α are produced primarily by the variation in the self-consistent field across the interface that is already present at equilibrium. DSCF theory quantifies the interfacial variations of the self-consistent field under non-equilibrium conditions, accounting for compressibility, spatial variations in the shear rate, and FENE-P chains.

The steady-state shear viscosity profiles in the interfacial

region for various chain lengths are calculated by dividing the viscous shear stress by the local shear rate and are shown in Fig. 3(a). Note that a drop in the viscosity occurs at the polymer-polymer interface, and it is more pronounced for longer chains. Corresponding results from MD are shown in Fig. 3(b). Here one can see that the trend predicted by the DSCF model is in general agreement with the MD results. The shear viscosities obtained from both methods in the bulk regions are very close. In the interfacial region, the drop is underestimated for long chains and slightly overestimated for short chains in the DSCF model, but the general agreement is very good given all the approximations of the model. A similar drop in the viscosity was also observed using MD [13], but with different parameters.

We have studied the interfacial slip phenomenon in phase-separated sheared polymer blends using the DSCF theory and compared our results with MD simulations. Good agreement between the two approaches is found. For unentangled polymer fluids studied here, the DSCF simulation time is only a small fraction of that in MD.

This work was supported by the Mitsubishi Chemical Corporation of Japan. M.M. and Y.S. would also like to acknowledge support by a grant from the National Science Foundation (Grant No. DMR-0080604). We would like to acknowledge useful discussions with Dr. G. Fredrickson and Dr. D. Wu. We thank Dr. T. Kawakatsu for sending his preprint prior to its publication.

- [1] J. Scheutjens and G. J. Fleer, *J. Phys. Chem.* **83**, 1619 (1979).
 [2] M. Mihajlovic, T. S. Lo, and Y. Shnidman, this issue, *Phys. Rev. E* **72**, 041801 (2005); M. Mihajlovic, Ph.D. thesis, Polytechnic University, 2004 (unpublished).
 [3] A. A. Khan and Y. Shnidman, *Prog. Colloid Polym. Sci.* **103**, 251 (1997).
 [4] N. M. Maurits, A. V. Zvelindovsky, and J. Fraaije, *J. Chem. Phys.* **109**, 11032 (1998); G. H. Fredrickson, *ibid.* **117**, 6810 (2002); T. Shima, H. Kuni, Y. Okabe, M. Doi, H. F. Yuan, and T. Kawakatsu, *Macromolecules* **36**, 9199 (2003).
 [5] B. Schmittmann and R. K. P. Zia, *Statistical Mechanics of Driven Diffusive Systems* (Academic Press, London, 1995).
 [6] R. Bird, C. Curtiss, R. Armstrong, and O. Hassager, *Dynamics of Polymeric Liquids*, 2nd ed. (Wiley, New York, 1987), Vol. 2.
 [7] M. Herrchan and H. C. Ottinger, *J. Non-Newtonian Fluid Mech.* **68**, 17 (1997).
 [8] A. K. Doolittle and D. B. Doolittle, *J. Appl. Phys.* **28**, 901 (1957).
 [9] K. Kremer and G. Grest, *J. Chem. Phys.* **92**, 5057 (1990).
 [10] A. N. Semenov, *Macromolecules* **27**, 2732 (1994); Martin-D. Lacasse, G. S. Grest, and A. J. Levine, *Phys. Rev. Lett.* **80**, 309 (1998); K. Binder, M. Muller, F. Schmid, and A. Werner, *Adv. Colloid Interface Sci.* **94**, 237 (2001).
 [11] P. G. de Gennes, *C.R. Acad. Sci., Ser. IIC: Chim* **308**, 1401 (1989); F. Brochard, P. G. de Gennes, and S. Troian, *ibid.* **310**, 1169 (1990).
 [12] J. L. Goveas and G. H. Fredrickson, *Eur. Phys. J. B* **2**, 79 (1998).
 [13] S. Barsky and M. O. Robbins, *Phys. Rev. E* **63**, 021801 (2001).
 [14] R. Zhao and C. W. Macosko, *J. Rheol.* **46**, 145 (2002).
 [15] S. Barsky and M. O. Robbins, *Phys. Rev. E* **65**, 021808 (2002).